1   **Metatranscriptomics supports mechanism for biocathode electroautotrophy by**

2   **"*Candidatus* Tenderia electrophaga"**

3

4   **Running title:**

5   *Ca.* **Tenderia electrophaga biocathode electroautotrophy**

6

7

8   Brian J. Eddie[1#], Zheng Wang[1], W. Judson Hervey IV[1], Dagmar H. Leary[1], Anthony P.

9   Malanoski[1], Leonard M. Tender[1], Baochuan Lin[1,2], Sarah M. Strycharz-Glaven[1]

10

11   [1]United States Naval Research Laboratory, 4555 Overlook Ave. SW, Washington, D.C. 20375

12   [2]Current address: Defense Threat Reduction Agency, 8725 John J Kingman Rd #6201, Fort

13   Belvoir, VA 22060

14   #To whom correspondence should be addressed: brian.eddie@nrl.navy.mil

15

16

ABSTRACT

Biocathodes provide a stable electron source to drive reduction reactions in electrotrophic microbial electrochemical systems. Electroautotrophic biocathode communities may be more robust than monocultures in environmentally relevant settings, but some members are not easily cultivated outside of the electrode environment. We previously used metagenomics and metaproteomics to propose a pathway for coupling extracellular electron transfer (EET) to carbon fixation in "*Candidatus* Tenderia electrophaga", an uncultivated but dominant member of the Biocathode-MCL electroautotrophic community. Here we validate and refine this proposed pathway using differential metatranscriptomics of replicate MCL reactors poised at the growth potential 310 mV and the suboptimal 470 mV (vs. standard hydrogen electrode). At both potentials, transcripts from "*Ca.* Tenderia electrophaga" were more abundant than from any other organism and its relative activity was positively correlated with current. Several genes encoding key components of the proposed "*Ca.* Tenderia electrophaga" EET pathway were more highly expressed at 470 mV, consistent with a need for cells to acquire more electrons to obtain the same amount of energy as at 310 mV. These included *cyc2*, encoding a homolog of a protein known to be involved in iron oxidation, confirmed to be differentially expressed by droplet digital PCR of independent biological replicates. Average expression of all CO_2 fixation related genes is 1.23-fold higher at 310 mV, indicating that reduced energy availability at 470 mV decreased CO_2 fixation. Our results substantiate the claim that "*Ca.* Tenderia electrophaga" is the key MCL electroautotroph, which will help guide further development of this community for microbial electrosynthesis.

IMPORTANCE

40

41 Bacteria that directly use electrodes as metabolic electron donors (biocathodes) have been

42 proposed for applications ranging from microbial electrosynthesis to advanced bioelectronics for

43 cellular communication with machines. However, just as we understand very little about

44 oxidation of analogous natural insoluble electron donors, such as iron oxide, the organisms and

45 extracellular electron transfer (EET) pathways underlying the electrode-cell direct electron

46 transfer processes are almost completely unknown. Biocathodes are a stable biofilm cultivation

47 platform to interrogate both the rate and mechanism of EET using electrochemistry and study the

48 electroautotrophic organisms that catalyze these reactions. Here we provide new evidence

49 supporting the hypothesis that the uncultured bacterium "*Candidatus* Tenderia electrophaga"

50 directly couples extracellular electron transfer to CO_2 fixation. Our results provide insight into

51 developing biocathode technology, such as microbial electrosynthesis, as well as advancing our

52 understanding of chemolithoautotrophy.

INTRODUCTION

53

54 Biocathodes are bioelectrochemical systems (BES) in which microbial electrode catalysts

55 use the electrode as an electron donor to drive cellular metabolism. Over the last decade

56 biocathodes have been explored for improving energy recovery in microbial fuel cells (MFCs),

57 electrode driven bioremediation, and more recently to produce chemicals in a process known as

58 microbial electrosynthesis (reviewed in (1, 2)). Despite widespread interest in biocathodes for

59 biotechnology applications, little is understood about the underlying mechanisms of extracellular

60 electron transfer (EET) for biocathode microorganisms. The *Marinobacter-Chromatiaceae-*

61 *Labrenzia* (MCL) biocathode is a self-regenerating, self-sustaining, aerobic microbial

62 community and has served in our lab as a model system for the exploration of electroautotrophic

3

63   microbial communities using an omics approach (3, 4). MCL forms a heterogeneously

64   distributed biofilm with clumps of up to 20 µm thick (4) with reproducible electrochemical

65   features following inoculation of a portion of the biofilm into a new reactor. It is proposed that

66   MCL, which operates under aerobic conditions, reduces O_2 with electrons supplied solely by the

67   cathode, directing a portion of the acquired energy and electrons for autotrophy. Cyclic

68   voltammetry (CV) reveals a sigmoid-shaped dependency for O_2 reduction catalytic (turnover)

69   current on electrode potential (5). It is proposed that this dependency reflects Nernstian behavior

70   of the heterogeneous electron transfer reaction (across the biofilm/electrode interface) that is

71   mediated by a redox cofactor, which is fast, reversible and not the rate limiting step in electron

72   uptake form the cathode by the biofilm (4, 6, 7). Electroautotrophic growth is assumed for MCL

73   based on an increase in biomass correlated to increasing current, a lack of organic carbon in the

74   bioelectrochemical reactor, and identification of an active Calvin-Benson-Bassham cycle (CBB)

75   (8). Electroautotrophic growth of isolates at potentials > -100 mV vs. SHE has thus far only

76   been demonstrated for *Mariprofundus ferrooxydans* PV-1 and *Acidithiobacillus ferrooxidans* (9,

77   10), while other autotrophs require supplemental energy from light or hydrogen for initial growth

78   on a cathode (11, 12). However, recent reports indicate that communities containing

79   *Gammaproteobacteria* using a high potential biocathode as an energy source can be reproducibly

80   enriched (13, 14).

81   Previous metagenomic and proteomics studies of MCL have led to the identification of

82   putative EET and CO_2 fixation mechanisms (8, 15) although efforts at cultivation have not

83   yielded the proposed electroautroph, "*Candidatus* Tenderia electrophaga" (16). Other work has

84   resulted in isolates from biocathode enrichments, but these have not been autotrophic (17, 18).

85   Metaproteomic analysis suggests that proteins that may be involved in EET are expressed at high

86   levels in the biofilm, including a homolog of Cyc2, a protein known to be involved in Fe^{+2}

87   oxidation in *A. ferrooxidans* (8). Subsequent metaproteomic analysis of the biofilm at two

88   different electrode potentials showed that some components of the electron transport chain

89   (ETC) are differentially expressed including an ortholog of Cyc1, thought to be involved in Fe^{+2}

90   oxidation in *M. ferrooxydans* PV-1 (19), and a hypothetical protein homologous to the terminal

91   oxidase cytochrome cbb_3 subunit CcoO (15). More precise quantification of the changes in gene

92   expression obtained using RNA-seq to quantify the relative abundance of transcripts (20) can be

93   used to understand the molecular mechanisms used for growth on the cathode.

94   Building upon our previous work (4, 8, 15), we applied RNA-seq to MCL to assess gene

95   expression of proposed EET and CO_2 fixation pathways for "*Ca.* Tenderia electrophaga" when

96   the applied electrode potential is adjusted from 310 mV vs. SHE (optimal for growth) to 470 mV

97   (suboptimal for growth). This 160 mV increase in potential decreases the $\Delta G^{0'}$ for the reduction

98   of O_2 by about one third, and from previous metaproteomic experiments run under identical

99   conditions is expected to result in changes in gene expression to compensate for the change in

100   energy availability. These results support previously hypothesized roles of some protein

101   complexes (8, 15, 19), and reveal possible EET roles for other proteins. We also provide further

102   evidence that "*Ca.* Tenderia electrophaga" is the keystone species in this community and is

103   strongly associated with current production. These results provide further understanding of the

104   molecular mechanisms involved in electroautotrophic growth on a cathode, enabling the use of

105   members of this community to develop biocathodes for applications including synthesis of value

106   added compounds or biofuels as well as potential ET components for microbial bioelectronics.

107   **<u>RESULTS</u>**

108   ***Biocathode-MCL Metatranscriptome:***

109   Eight BES were grown under previously described standard conditions at an applied

110   electrode potential of 310 mV SHE. Seven of the eight biological replicates reached maximum

111   current production within five days (Table 1, Fig. S1). Replicate S2A took two days longer. The

112   midpoint potential (E_M) of each BES measured by cyclic voltammetry (CV) once steady-state

113   current was achieved was identical to that previously reported (4, 8, 15) at ca. 440 mV vs. SHE

114   (Table 1). Following CV, the electrode potential was either returned to 310 mV or adjusted to

115   470 mV, a potential at which we expect the biofilm to recover less energy per electron based on

116   previous experiments.

117   MiSeq mRNA sequencing yielded between 4.5 – 16.2 million reads per replicate sample

118   that passed quality control steps and were used for read alignment to the metagenome, of which

119   37.9-87.5% could be unambiguously aligned (Table 1). The relative activity of MCL constituents

120   was assessed as the proportion of reads mapping to a metagenome bin normalized by relative

121   length of bin. Using this metric, MCL constituents previously implicated in key roles in the

122   biocathode – "*Ca.* Tenderia electrophaga", *Marinobacter* sp. strain CP1, and *Labrenzia* sp. strain

123   CP4. – were highly active in all samples at both potentials. Ten other metagenome bins were

124   active in all eight samples using a cutoff of 0.01% of relative activity. Two of these,

125   *Parvibaculum* sp. and *Kordiimonas* sp. had activity similar to that of *Labrenzia* sp. and

126   *Marinobacter* sp., indicating that they may also have significant roles in the biocathode

127   community. "*Ca.* Tenderia electrophaga" was the most active organism in all eight samples,

128   comprising 53% to 84.3% of activity (Fig. 1). *Marinobacter* sp., *Labrenzia* sp., *Kordiimonas*

129   sp., and *Parvibaculum* sp. average 24.6% of the remaining activity. These five organisms make

130   up the core of the biofilm community, on average accounting for 93.6% of community activity.

131   Two-tailed Student's T-tests indicated that no organism has a significant change in activity

132   between the two potentials tested ($p > 0.09$ for all bins).

133   ***Correlation of "Ca. Tenderia electrophaga" transcriptional activity to current density***

134   Activity of "*Ca.* Tenderia electrophaga" was strongly correlated to current density at both

135   310 mV and 470 mV (Fig. 2A) with Pearson correlation coefficients of 0.975 and 0.967

136   respectively. Activity of the four most active heterotrophic organisms, *Labrenzia* sp.,

137   *Marinobacter* sp., *Parvibaculum* sp., and *Kordiimonas* sp. was negatively correlated, or not

138   correlated with current density (Fig. 2B-D). Previous metagenomic and metaproteomic data

139   indicated that "*Ca.* Tenderia electrophaga" is likely an autotrophic organism capable of

140   performing EET (8, 15) and the correlation of current density to activity supports this theory.

141   For this reason, we concentrated our analysis of metatranscriptomics data on "*Ca.* Tenderia

142   electrophaga" to focus specifically on how direct EET is linked to CO_2 fixation.

143   ***Different Pathways for Electron Transport Are Used at Different Potentials:***

144   Previous metagenomic and metaproteomic analysis of Biocathode-MCL revealed

145   proteins for carbon fixation through the CBB cycle and a putative EET pathway in "*Ca.* Tenderia

146   electrophaga" (8). Statistical analysis of protein expression revealed that nine proteins in "*Ca.*

147   Tenderia electrophaga" were detected more often at one potential versus another, but

148   methodological limitations meant that this was likely to be a small fraction of the response to

149   changing potential (15). Efforts to cultivate a representative isolate of "*Ca.* Tenderia

150   electrophaga" from MCL have thus far been unsuccessful, suggesting that other community

151   constituents satisfy unknown requirements for its growth. We therefore used metatranscriptomics

152   to obtain higher resolution analysis of differentially expressed mRNA levels for proteins

153   suspected to be involved in electroautotrophic growth. This allowed us to test the hypothesis that

154   expression of protein coding genes involved in respiration and energy flux in the primary

155   electroautotroph is directly influenced by the potential of electrons supplied by the cathode. A

156   complete list of genes we propose to be associated with these pathways is presented in Table S1.

157   Electrochemical measurements indicate redox dependent direct electron transfer (DET) is

158   occurring between the electrode and "*Ca.* Tenderia electrophaga" (4, 5), therefore, we searched

159   the metatranscriptome for evidence of an EET conduit whose expression may be affected by the

160   change in electrode potential. The *cyc*2 homolog in "*Ca.* Tenderia electrophaga" (Tel_03480)

161   was predicted to have a role in EET (8) based on its proposed involvement in iron oxidation and

162   was significantly differentially expressed, with relative transcript levels 1.8-fold higher at 470

163   mV. The gene for a predicted hexaheme lipoprotein (Tel_04230) was significantly more highly

164   expressed at 470 mV, raising the possibility that this protein is involved in electron transfer. An

165   undecaheme *c*-cyt (Tel_16545) was previously identified as a possible route for EET in "*Ca.*

166   Tenderia electrophaga" due to the large number of predicted heme binding sites, known to be

167   important for EET in *Shewanella* and *Geobacter spp.*, and its conservation among other EET

168   capable organisms (8). The gene for this protein was not differentially expressed.

169   It is thought that soluble, periplasmic cytochromes mediate ET between the outer

170   membrane and the cytoplasmic membrane bound ETC (21, 22). Several genes previously noted

171   from "*Ca.* Tenderia electrophaga" which may encode proteins involved in transferring electrons

172   across the periplasm to ETC were examined for changes in expression between the two electrode

173   potentials. Expression was higher for three tri-heme cytochromes (Tel_16515, Tel_16520,

174   Tel_16530) at 310 mV, but was not statistically significant ($p > 0.01$). Overall, these genes are

175   among the most highly expressed in "*Ca.* Tenderia electrophaga", indicating their importance for

8

176   growth at the cathode. They also appear to be co-transcribed with a gene encoding a

177   tetratricopeptide repeat (Tel_16525), which are known to be involved in protein:protein

178   interaction and may be involved in aligning cytochromes in a bridge configuration as proposed

179   for other EET capable bacteria (23). Peptides from this tetratricopeptide repeat protein were

180   previously found to be significantly more abundant at the suboptimal potential (15), although in

181   the metatranscriptomic data, this cluster of genes is slightly more highly transcribed at 310 mV.

182   A di-heme cytochrome c_4, Cyc1, has been proposed to be a periplasmic electron shuttle

183   in the iron oxidizing bacterium *M. ferrooxydans* (19). The gene encoding this protein is found in

184   "*Ca.* Tenderia electrophaga", in a region displaying synteny with two contigs from the *M.*

185   *ferrooxydans* genome (Figure S2). Like the tri-heme cytochromes, it is very highly expressed at

186   both potentials, but is not significantly differentially expressed. Other genes for potential

187   periplasmic electron carriers identified from the metatranscriptome that were not previously

188   implicated in MCL EET included a monoheme *c*-cyt (Tel_12755). This gene has the largest

189   change in expression of any annotated cytochrome in "*Ca*. Tenderia electrophaga" (3-fold more

190   highly expressed at 310 mV) suggesting that it may be important for electron transfer at this

191   lower potential. It is homologous to genes for proteins in several iron oxidizing bacteria,

192   including *Sideroxydans* (45% amino acid identity), *Gallionella* (42% identity), and

193   *Acidithiobacillus* (42% identity) species. This may make it an important gene to consider in

194   models of iron oxidation.

195   Regardless of the pathway used, e$^-$ need to reach the cytoplasmic membrane bound ETC,

196   which is the main mechanism for conservation of energy via chemiosmotic gradient formation

197   (24). Metatranscriptomic analysis of the ETC components does not indicate large changes in the

198   expression of these genes, which suggests that the same ETC components are used at both

199   electrode potentials. Small (<1.3 fold) changes in the ratios of expression for whole pathways

200   may represent subtle adjustments in the ratio of electrons going down each path (Table S1).

201   Whether this is in addition to or instead of the pathway being selected by potential of the electron

202   donor in a manner reminiscent of recent work on electron acceptors in *Geobacter sulfurreducens*

203   remains to be determined (25, 26).

204   Most genes encoding components of the ETC were not significantly differentially

205   expressed, although many had smaller but consistent changes in expression between the two

206   potentials. For example, the genes encoding the Alternative Complex III (ACIII), the

207   NADH:ubiquinone oxidoreductase complex (NUOR), and a homolog of Cyc1 from *M.*

208   *ferrooxydans*, thought to be responsible for transferring electrons from the outer membrane to the

209   cytochrome cbb_3 oxidase (19), were not differentially expressed. However, hierarchical

210   clustering based upon the slight changes of expression among these complexes (Fig. 3) suggests

211   that they are functionally linked. This supports a role as the reverse electron transport (RET)

212   chain, linking EET to the reduction of $NAD(P)^+$ for fixation.

213   Only one operon in "*Ca.* Tenderia electrophaga" contains all four of the canonical genes

214   for a bacterial cytochrome cbb_3 oxidase (*ccoNOPQ*), but it has relatively low expression.

215   However, the genome also encodes several proteins homologous to terminal oxidases (Complex

216   IV) that could potentially reduce O_2 and generate proton motive force (PMF). Of these, the

217   genes encoding Complex IV-2 had some of the highest total expression of any genes, and

218   clustered with the undecaheme cytochrome and two additional copies of *ccoO* (Fig. 3) which

219   suggests that this represents a way for electrons to enter the cell and be used to reduce O_2.

220   Among genes with a large change in expression, *cyc2* clustered with a gene cluster

221   encoding a possible nitrate reductase and a complex including a *ccoO* homolog and a copper

222   containing plastocyanin homolog labeled as Putative Complex IV. However, this cluster of

223   genes lacks a protein that could function as an analog of the membrane associated proton

224   pumping CcoN. Thus it is unlikely to make a substantial contribution to PMF. All of the genes

225   encoding components of the two ATP synthase operons were more highly expressed at 310 mV,

226   many with a false discovery rate (FDR) of <0.01, indicating that energy levels in "*Ca.* Tenderia

227   electrophaga" are dependent upon the electrode potential.

228   Expression of 19 genes was quantified using droplet digital-PCR (ddPCR) to verify

229   differential expression of several genes hypothesized to be important for growth on the cathode

230   (Table S2). These measurements we performed on an independent set of eight MCL

231   biocathodes, approximately one year after the original reactors. Only *cyc2* was found to be

232   differentially expressed in the both ddPCR results and the metatranscriptome. Variability

233   between inocula and the lack of an adequate method for normalizing to account for differences in

234   the biofilm community may have reduced the sensitivity of the assay.

Effect of potential on carbon fixation and central carbon metabolism:

236   The "*Ca.* Tenderia electrophaga" genome contains all the genes necessary for CO_2

237   fixation via the CBB cycle, including two forms of Rubisco – one associated with carboxysomes

238   (Form IAc) and one not associated with carboxysomes (Form IAq) (8). The lower energy yield

239   per electron from a cathode poised at 470 mV would result in less energy available for CO_2

240   fixation, so the central carbon metabolism of "*Ca.* Tenderia electrophaga" was examined for

241   changes in expression. Genes which could be involved in more than one pathway, for example,

242   CO_2 fixation and the pentose phosphate pathway, were separated where possible by examining

243   co-localization and changes in expression between the eight samples. Genes with ambiguous

244   functional roles that could not be assigned to a single pathway were excluded from this analysis.

11

245 Most components of central carbon metabolism, including the CBB cycle were more highly

246 expressed at 310 mV, although the absolute magnitude of the change was relatively small (Fig. 4,

247 Table S3). Only four genes were differentially expressed, ribose 5-phosphate isomerase A and

248 ribulose-phosphate 3-epimerase which catalyze anaplerotic reactions in the CBB cycle, and 6-

249 phosphogluconate dehydrogenase and glucose-6-phosphate 1-dehydrogenase which catalyze

250 components of the pentose phosphate pathway that supply metabolic precursors for biosynthesis.

251 However, when examining all genes in a given pathway, they were mostly consistent, indicating

252 that the pathways are likely genuinely more highly expressed. The exceptions are the form IAc

253 Rubisco genes and carboxysome genes. These were more highly expressed at 470 mV, which

254 suggests a switch to a more efficient enzyme under energy limitation. The whole CBB CO_2

255 fixation cycle was 1.23-fold more highly expressed at 310 mV.

256 **DISCUSSION**

257   Our characterization of the Biocathode-MCL community by metatranscriptomics agrees

258 with previous metaproteomic and 16S rRNA amplicon characterization of Biocathode-MCL that

259 there is substantial variability in the abundance of specific bacteria, even between seemingly

260 identical reactors inoculated on the same day with the same inoculum (15). However, as in the

261 previous studies, changing the electrode potential from 310 mV to 470 mV for 52 hours after the

262 community had developed did not result in significant changes in the average relative abundance

263 of biocathode constituents between the two potentials. While the inherent variability in relative

264 abundance between replicate reactors makes analysis of the transcriptome data challenging,

265 differences that we found are more likely to be robust because they are visible above the noise of

266 such large biological variability when using paired, replicated samples as in Leary et al. (15).

267   The magnitude of changes in gene expression were relatively small compared to other

268   transcriptomic studies (e.g. (27, 28)). However, in one of those studies, replicate samples were

269   acquired by repeatedly sampling the same biofilm, which may have inflated the reported

270   statistical confidence, and in the other no replicates were sampled. The 52 hours adjustment

271   period after changing the potential likely decreased the magnitude of the transcriptional

272   response, but it was chosen to facilitate comparison to proteomics data (15). On a shorter

273   timescale, transcription of genes for upregulated pathways may experience a burst, as the cells

274   adjust to the new regulatory regime, but would relax back to the new steady state once the proper

275   balance of proteins has been reached. Also, the fundamental metabolism of "*Ca.* Tenderia

276   electrophaga" does not change. Electrons are still being transferred from the cathode to the ETC,

277   and CO_2 fixation is still the sole carbon source.

278   Our results suggest that "*Ca.* Tenderia electrophaga" is primarily responsible for EET

279   linked to CO_2 fixation in Biocathode-MCL biofilms. The dominance of "*Ca.* Tenderia

280   electrophaga" transcriptional activity and its correlation to current density suggests that it can

281   account for the majority of current. Further substantiating this hypothesis is the recent repeated

282   identification of unclassified bacteria, thought to be within the *Chromatiales,* which were

283   dominant members of freshwater biocathode communities (13, 14). While *Marinobacter* spp.

284   are capable of cathode oxidation (17, 18, 29), isolates of *Marinobacter* sp. and *Labrenzia* sp.

285   from the MCL-community are only capable of weak current production at the biocathode or iron

286   oxidation in monoculture (8).

287   Based on a prior analysis of Biocathode-MCL using low scan rate CV, we predicted

288   current to be approximately halved when the electrode potential was switched from 310 mV to

289   470 mV (15). However, as previously observed (15), for biocathode-MCL, switching to and

13

290   maintaining a more positive potential (470 mV) over a much longer time period (>50 h) resulted

291   in an increase in current attributed to O_2 reduction after the initial adjustment period. This

292   increase in current is interpreted as the result of the need to make up for the decrease in energy

293   available per electron at the higher potential. Using a derivation of the Nernst Equation ($\Delta G =$

294    $nF\Delta E^{0'}$) to estimate the theoretical yield of O_2 reduction to H_2O using an electron donor at a

295   potential of 310 mV, yields -47 kJ/mol e^-, requiring an additional ~61 kJ/mol e^- to reduce

296    $NAD(P)^+$. Assuming that the energy required to pump protons across the membrane is ~21

297   kJ/mol, at the optimal potential "*Ca.* Tenderia electrophaga" could export two H^+ per e^-, and

298   would need to use three H^+ to reduce $NAD(P)^+$. This results in a theoretical balance for electron

299   utilization by the forward vs. reverse electron transport pathways of ~ 60%/40% to produce

300   NAD(P)H. More electrons would need to go to the forward path to generate a proton gradient

301   for ATP production. In comparison, using an electron donor at a potential of 470 mV reduces

302   the ΔG to -32 kJ/mol e^-, lowering the theoretical yield to ~1.5 H^+ exported per e^-, and the larger

303    $\Delta E^{0'}$ between the electrode and NAD(P)H requires at least four H^+ translocated per $NAD(P)^+$

304   reduced. This results in a balance of at least 80% and 20% for the electron utilization by the

305   forward and reverse pathways. Thus, theoretically, at least twice as many electrons are needed to

306   generate the same amount of reducing equivalents for CO_2 fixation at the more positive potential.

307   During growth in standard culture conditions, the acidophilic iron oxidizer *A. ferrooxidans* is

308   predicted to have a ratio closer to 90/10% for the forward vs. reverse pathways, including the

309   proton gradient necessary to generate ATP (30). Recent experimental evidence suggests that

310   during growth on an electrode, the ratio of electron utilization by the forward to reverse

311   pathways is close to 15:1 in *A. ferrooxidans* (10).

312   The majority of CBB cycle genes and pentose phosphate cycle genes appear to be more

313   highly expressed at 310 mV. This likely reflects a higher rate of CO_2 fixation at 310 mV

314   compared to 470 mV. Furthermore, the higher relative expression of the Form IAc Rubisco

315   genes and their associated carboxysomes at 470 mV may reflect the need to increase the

316   efficiency of CO_2 fixation due to the lower energy availability. However, even at 470 mV, the

317   overall transcript abundance of Form IAq is still twice as high as Form IAc.

318   Among components possibly involved in ET at the outer membrane, the Cyc2 homolog

319   encoded by Tel_03480 was more highly expressed at 470 mV in both metatranscriptomic and

320   ddPCR samples, consistent with the lower energetic yield per electron. This protein has

321   previously been implicated in EET in the acidophilic iron oxidizing bacterium *A. ferrooxidans*

322   ATCC19859 (31-33). The E_M of Cyc2 in *A. ferrooxidans* is reported to be 560 mV at pH 4.8

323   (23). This is within the range that might be expected for a protein accepting electrons from a

324   cathode at the potentials tested, although the midpoint potential of Cyc2 in "*Ca.* Tenderia

325   electrophaga" is likely different. This strongly suggests that Cyc2 is involved in EET with the

326   electrode in "*Ca.* Tenderia electrophaga", although its exact role given the single heme and lack

327   of transmembrane helices remains unknown.

328   Redundancy of electron transport chain components suggests large amount of metabolic

329   flexibility in "*Ca.* Tenderia electrophaga" depending upon potentials of electron donors and local

330   redox environment (Fig. 5). Thermodynamics dictates that the balance of electrons passing

331   through the two branches of the ETC depends upon the electrode potential. One possible method

332   of controlling this ratio would be modulating the abundance of the periplasmic links between

333   EET and the ETC. Several proteins could potentially make up this link, but their roles are

334   presently unclear. Hierarchical clustering of potential electron transfer components by

15

335   expression leads to several distinct clusters (Fig. 3). One cluster contains the ACIII and Complex

336   I genes, which suggests that these complexes may be functionally linked. This cluster also

337   contains the Cyc1 homolog which suggests that it may facilitate the transfer of electrons to the

338   "uphill" ETC, rather than to the terminal oxidase as proposed elsewhere (19, 30). The canonical

339   cytochrome cbb_3 oxidase is part of a cluster with succinate dehydrogenase (Complex II) and the

340   cytochrome bc_1 complex. This may indicate that they form part of a forward ETC, which would

341   enable the use of stored reserves in the form of glycogen.

342   Metatranscriptomics supports previous work by our group that identified "*Ca.* Tenderia

343   electrophaga" as the electroautotroph. It appears to be the key member of the community and its

344   predicted lifestyle as an electroautotroph is supported by a several key findings. "*Ca.* Tenderia

345   electrophaga" was more active than any other organism and its activity was positively correlated

346   with current density. Genes for proteins previously predicted to be involved in EET in "*Ca.*

347   Tenderia electrophaga"*,* including Cyc2, were more highly expressed at 470 mV, when more

348   electrons are needed to generate the same amount of PMF. The membrane bound ETC that is

349   necessary to generate the ATP and reducing power for CO_2 fixation was active at both potentials,

350   but a potential complex IV analog and several that may be involved in the "downhill" branch of

351   the ETC showed increased expression in response to changes in electrode potential. These

352   changes were consistent with the need to use more electrons to obtain the same amount of

353   energy. Most components of central carbon metabolism found were more highly expressed at

354   310 mV, suggesting a higher metabolic rate. The evidence for involvement of specific proteins

355   or complexes in EET and ETC is correlative in nature, but narrows the list of potential targets for

356   future confirmatory studies that are in progress. Further investigations with better temporal

357   resolution may yield additional insights into the dynamics of the response to the changes in

358   potential. Heterologous expression and biochemical measurements of predicted components of

359   EET and the ETC may help identify functional roles. This work provides insight into the

360   mechanisms for electroautotrophic growth in this biocathode community that will assist in

361   engineering biocathode communities.

METHODS

363   **Biofilm growth and sampling:**

364   Samples for RNA-seq were grown in artificial seawater medium (ASW) as previously

365   described (8). Inocula consisted of cells detached from a 3 cm x 3 cm portion of a carbon cloth

366   electrode and counted using an Accuri C6 flow cytometer (BD Bioscience, San Jose, CA)

367   described previously (15). Sterile 2 L dual chambered microbial fuel cell reactors (Adams and

368   Chittenden Scientific Glass) reactors containing a graphite coupon 3 cm x 9 cm x 0.2 cm were

369   inoculated with standardized inocula estimated to contain 2×10^5 cells.

370   Four reactors were inoculated with the same inoculum and grown under standard

371   conditions (310 mV SHE), until they reached the maximum current (12 - 65 mA m^{-2}). At this

372   point, cyclic voltammetry (CV) was CV recorded from 610 mV to 260 mV and back to 610 mV

373   at a scan rate of 0.2 mV/s. After CV, two reactors remained poised at 310 mV, and two were

374   shifted to a suboptimal potential (470 mV SHE) where CV indicates that the rate of electron

375   uptake is approximately half of that at the "optimal" potential. After 52 hours, the biofilm was

376   scraped from ~3 x 9 cm portions of both sides of the cathode with a sterile razor blade,

377   immediately immersed in RNA*later*® (life Technologies, Grand Island, NY) and stored at 4° C

378   overnight prior to freezing at -20°C until total RNA extraction. This experiment was repeated 7

379   days later with a new inoculum. This gave two pairs of biological replicates for each treatment.

RNA extraction, library prep, and sequencing:

380

381   Biofilm RNA were extracted using an established protocol (34) with the following

382   modification, instead of 0.8 g of 0.5 mm glass beads, 250 µL of Zirconia beads (Life

383   Technologies) were used. The extracted RNA samples were subject to DNase treatment using

384   Turbo DNase (Life Technologies) and cleaned up using RNA clean & concentrator^{TM}-5 (Zymo

385   Research). The DNase treatment was repeated once for each sample to ensure the removal of

386   contaminating DNA. Ribosomal RNA was depleted from RNA samples using Ribo-Zero rRNA

387   Removal Kit for Bacteria (Illumina, San Diego, CA). RNA library preparation was carried out

388   using NEBNext® Ultra RNA^{TM} Library Prep Kit for Illumina (New England Biolabs, Inc.,

389   Ipswich, MA) according to the manufacturer's recommended protocol. The sequence reads of

390   RNA libraries were acquired on a MiSEQ^{TM} instrument under automated software control

391   (version 2.2.0, Illumina, San Diego, CA). Raw reads that passed the initial quality filter were

392   submitted to the NCBI Short Read Archive (http://www.ncbi.nlm.nih.gov/bioproject) under

393   Bioproject PRJNA244670 experiment SRX978937 objects SAMN03462067 - SAMN03462074.

Metatranscriptome alignment and statistical analysis of gene expression:

394

395   Metatranscriptome reads were trimmed for quality using Trimmomatic 0.30 with a

396   sliding window set to 5 bases with a minimum score of 25 and the first eight bases of the

397   sequence and any leading bases with a quality score less than 20 were cropped (35). Reads

398   shorter than 50 bases were discarded. To avoid inflated statistical confidence, only read one of

399   the paired end reads was used, and if read one had been discarded during trimming, read two was

400   used. Bowtie 2 (36) was used to align reads to the Biocathode-MCL metagenomic assembly

401   available at http://www.ncbi.nlm.nih.gov under Bioproject PRJNA244670 (Malanoski et al. in

18

402 prep), modified by removing contigs from the bins corresponding to PacBio sequenced genomes

403 of "*Ca.* Tenderia electrophaga", *Labrenzia* sp. CP4, and *Marinobacter* sp. CP1 (CP013099.1,

404 CP013100.1, CP011929.1, CP011927.1, and CP011928.1) and contigs with >98% identical over

405 >90% of their length. Single-end mode was used with the following options: -D 30 -R 3 -N 1 -L

406 15-i S,1,0.50 --score-min L,0,-0.15.

407   Read counts per contig were calculated using the idxstats function in samtools (37).

408 Relative activity of each genome or metagenomic bin was calculated as the sum of RNA-seq

409 reads mapping to the genome or bin divided by length of the genome or bin in nucleotides as a

410 percent of activity in the library. Read counts per gene were calculated with HTseq-count.

411 EdgeR (38, 39) was used to determine the statistical significance of differences in read counts for

412 each annotated gene and pseudogene in "*Ca.* Tenderia electrophaga" with Benjamini-Hochberg

413 adjustment to reduce the false discovery rate due to multiple hypothesis testing (40). A

414 multifactor experimental design was used to separate changes in expression likely to be due to

415 the different inocula from changes in expression resulting from the change in electrode potential

416 (41). The sensitivity of this method to sequence coverage meant that a much smaller change in

417 relative abundance of mRNAs was needed to reach the same FDR for genome bins with high

418 coverage depth. Thus, the FDR used to determine a differentially expressed gene was FDR <

419 0.01. Values reported for gene expression at each condition are $\log_2$ of the number of reads per

420 gene after normalization and variance stabilization transformation (42) (Table S4). Overall gene

421 expression was calculated as EdgeR normalized gene expression minus the $\log_2$ of the length of

422 the gene. For clustering genes by change in expression, gene expression was centered at 0 for

423 each inoculum. Euclidean distance matrices were calculated, and genes were clustered using the

424 Ward method implemented in the R package "pheatmap" version 0.7.7 (43).

425   Correlations between current density and relative abundance of mRNA from each

426   metagenomic genome or bin were calculated as Pearson's product moment correlation

427   coefficient (44). The critical value for a significant correlation for a two-tailed test with a sample

428   size of n = 4 is 0.9 for a p-value of 0.1. A higher p-value cutoff for the correlation is justified

429   because this is a different kind of statistical test and it assumes a linear relationship between the

430   data, which is likely not the case for most genes. Furthermore, there is a large variability

431   between samples of the same conditions (current magnitude, current increasing/decreasing, and

432   community composition) that would prevent the near perfect correlation a p-value of 0.01 would

433   require.

434   **Validation of differential expression with ddPCR:**

435   RNA samples from eight additional biological replicates were obtained from the same

436   inoculum following the protocol above (four optimal and four suboptimal). After RNA

437   extraction, a whole transcriptome amplification protocol was applied using the WTA-2 kit

438   (Sigma) according to the manufactures instructions, performing a no template negative control.

439   Individual ddPCR reactions for each primer set listed in Table S5 were set up using QX200

440   ddPCR EvaGreen Supermix (BioRad) and QX200 Droplet Generation Oil for EvaGreen

441   (BioRad). Copy numbers of mRNAs for 19 genes were assessed as copy number per µl of

442   reaction minus calculated copy number per µl of corresponding negative control reaction.

443   Samples were normalized using a trimmed means approach to account for variation in the

444   proportion of "*Ca.* Tenderia electrophaga" in the community, and significance of differential

445   expression was assessed using two-tailed t-tests.

446   **Accession number(s):**

447   All sequences produced in this study are available in the NCBI Short Read Archive under

448   Bioproject number: PRJNA244670

Acknowledgements:

Funding information:

References:

460   1.   **Tremblay P-L, Zhang T.** 2015. Electrifying microbes for the production of chemicals. Front

461   Microbiol **6**.10.3389/fmicb.2015.00201.

462   2.   **Rabaey K, Rozendal RA.** 2010. Microbial electrosynthesis - revisiting the electrical route for

463   microbial production. Nat Rev Microbiol **8:**706-716.10.1038/nrmicro2422.

464   3.   **Malik S, Drott E, Grisdela P, Lee J, Lee C, Lowy DA, Gray S, Tender LM.** 2009. A self-

465   assembling self-repairing microbial photoelectrochemical solar cell. Energy Environ Sci **2:**292-

466   298

467 4. **Strycharz-Glaven SM, Glaven RH, Wang Z, Zhou J, Vora GJ, Tender LM.** 2013.

468   Electrochemical Investigation of a Microbial Solar Cell Reveals a Nonphotosynthetic Biocathode

469   Catalyst. Appl Environ Microbiol **79:**3933-3942.10.1128/Aem.00431-13.

470 5. **Yates MD, Eddie BJ, Kotloski NJ, Lebedev N, Malanoski AP, Lin B, Strycharz-Glaven SM,**

471   **Tender LM.** (Accepted 2016). Understanding Long-Distance Extracellular Electron Transport in

472   an Electroautotrophic Microbial Community. Energy Environ Sci

473 6. **Strycharz SM, Malanoski AP, Snider RM, Yi H, Lovley DR, Tender LM.** 2011. Application

474   of cyclic voltammetry to investigate enhanced catalytic current generation by biofilm-modified

475   anodes of Geobacter sulfurreducens strain DL1 vs. variant strain KN400. Energy Environ Sci

476   **4:**896-913.10.1039/C0EE00260G.

477 7. **Torres CI, Marcus AK, Lee H-S, Parameswaran P, Krajmalnik-Brown R, Rittmann BE.**

478   2010. A kinetic perspective on extracellular electron transfer by anode-respiring bacteria. FEMS

479   Microbiol Rev **34:**3-17

480 8. **Wang Z, Leary DH, Malanoski AP, Li RW, Hervey WJ, Eddie BJ, Tender GS, Yanosky**

481   **SG, Vora GJ, Tender LM, Lin B, Strycharz-Glaven SM.** 2015. A Previously Uncharacterized,

482   Nonphotosynthetic Member of the *Chromatiaceae* Is the Primary CO_2-Fixing Constituent in a

483   Self-Regenerating Biocathode. Appl Environ Microbiol **81:**699-712.10.1128/aem.02947-14.

484 9. **Summers ZM, Gralnick JA, Bond DR.** 2013. Cultivation of an obligate Fe(II)-oxidizing

485   lithoautotrophic bacterium using electrodes. MBio **4:**e00420-00412.10.1128/mBio.00420-12.

486 10. **Ishii T, Kawaichi S, Nakagawa H, Hashimoto K, Nakamura R.** 2015. From

487   Chemolithoautotrophs to Electrolithoautotrophs: CO_2 Fixation by Fe (II)-Oxidizing Bacteria

488   Coupled with Direct Uptake of Electrons from Solid Electron Sources. Front Microbiol **6:**994

489 11. **Nevin KP, Hensley SA, Franks AE, Summers ZM, Ou J, Woodard TL, Snoeyenbos-West**

490   **OL, Lovley DR.** 2011. Electrosynthesis of Organic Compounds from Carbon Dioxide Is

491   Catalyzed by a Diversity of Acetogenic Microorganisms. Appl Environ Microbiol **77:**2882-

492   2886.10.1128/aem.02642-10.

493   12.   **Bose A, Gardel EJ, Vidoudez C, Parra EA, Girguis PR.** 2014. Electron uptake by iron-

494   oxidizing phototrophic bacteria. Nat Commun **5:**3391.10.1038/ncomms4391.

495   13.   **Rothballer M, Picot M, Sieper T, Arends JB, Schmid M, Hartmann A, Boon N, Buisman C,**

496   **Barrière F, Strik DP.** 2015. A monophyletic group of unclassified γ-Proteobacteria dominates in

497   a mixed culture biofilm of high-performing oxygen reducing biocathode. Bioelectrochemistry

498   14.   **Desmond-Le Quéméner E, Rimboud M, Bridier A, Madigou C, Erable B, Bergel A,**

499   **Bouchez T.** 2016. Biocathodes reducing oxygen at high potential select biofilms dominated by

500   *Ectothiorhodospiraceae* populations harboring a specific association of genes. Bioresour Technol

501   **214:**55-62

502   15.   **Leary DH, Hervey JW, Malanoski AP, Wang Z, Eddie BJ, Tender GS, Vora GJ, Tender**

503   **LM, Lin B, Strycharz-Glaven SM.** 2015. Metaproteomic evidence of changes in protein

504   expression following a change in electrode potential in a robust biocathode microbiome.

505   Proteomics doi:10.1002/pmic.201400585**:**3486–3496.10.1002/pmic.201400585.

506   16.   **Eddie BJ, Wang Z, Malanoski AP, Hall RJ, Oh SD, Heiner C, Lin B, Strycharz-Glaven SM.**

507   2016. '*Candidatus* Tenderia electrophaga', an uncultivated electroautotroph from a biocathode

508   enrichment. Int J Syst Evol Microbiol **66:**2178-2185.doi:10.1099/ijsem.0.001006.

509   17.   **Debuy S, Pecastaings S, Bergel A, Erable B.** 2015. Oxygen-reducing biocathodes designed with

510   pure cultures of microbial strains isolated from seawater biofilms. Int Biodeterior Biodegrad

511   **103:**16-22

512   18.   **Rowe AR, Chellamuthu P, Lam B, Okamoto A, Nealson KH.** 2014. Marine sediments

513   microbes capable of electrode oxidation as a surrogate for lithotrophic insoluble substrate

514   metabolism. Front Microbiol **5.** doi: 10.3389/fmicb.2014.00784

515   19.   **Barco RA, Emerson D, Sylvan JB, Orcutt BN, Meyers MEJ, Ramírez GA, Zhong JD,**

516   **Edwards KJ.** 2015. New Insight into Microbial Iron Oxidation as Revealed by the Proteomic

517   Profile of an Obligate Iron-Oxidizing Chemolithoautotroph. Appl Environ Microbiol **81:**5927-

518   5937

23

20. **Nagalakshmi U, Wang Z, Waern K, Shou C, Raha D, Gerstein M, Snyder M.** 2008. The transcriptional landscape of the yeast genome defined by RNA sequencing. Science **320:**1344-1349

21. **Pokkuluri PR, Londer YY, Duke NE, Long WC, Schiffer M.** 2004. Family of cytochrome c 7-type proteins from Geobacter sulfurreducens: structure of one cytochrome c 7 at 1.45 Å resolution. Biochemistry **43:**849-859

22. **Bird LJ, Bonnefoy V, Newman DK.** 2011. Bioenergetic challenges of microbial iron metabolisms. Trends Microbiol **19:**330-340.10.1016/j.tim.2011.05.001.

23. **Castelle C, Guiral M, Malarte G, Ledgham F, Leroy G, Brugna M, Giudici-Orticoni M-T.** 2008. A new iron-oxidizing/O2-reducing supercomplex spanning both inner and outer membranes, isolated from the extreme acidophile *Acidithiobacillus ferrooxidans*. J Biol Chem **283:**25803-25811

24. **Mitchell P.** 1961. Coupling of phosphorylation to electron and hydrogen transfer by a chemi-osmotic type of mechanism. Nature **191:**144-148

25. **Levar CE, Hoffman CL, Dunshee AJ, Toner BM, Bond DR.** 2016. Redox potential as a master variable controlling pathways of metal reduction by *Geobacter sulfurreducens*. bioRxiv doi:10.1101/043059.10.1101/043059.

26. **Zacharoff L, Chan CH, Bond DR.** 2016. Reduction of low potential electron acceptors requires the CbcL inner membrane cytochrome of *Geobacter sulfurreducens*. Bioelectrochemistry **107:**7-13

27. **Ishii Si, Suzuki S, Norden-Krichmar TM, Tenney A, Chain PS, Scholz MB, Nealson KH, Bretschger O.** 2013. A novel metatranscriptomic approach to identify gene expression dynamics during extracellular electron transfer. Nature communications **4:**1601

28. **Marshall C, Ross D, Handley K, Weisenhorn P, Edirisinghe J, Henry C, Gilbert J, May H, Norman RS.** 2016. Metabolic Reconstruction and Modeling Microbial Electrosynthesis. bioRxiv doi:10.1101/059410.10.1101/059410.

545   29.   **Vandecandelaere I, Nercessian O, Faimali M, Segaert E, Mollica A, Achouak W, De Vos P,**

546   **Vandamme P.** 2010. Bacterial diversity of the cultivable fraction of a marine electroactive

547   biofilm. Bioelectrochemistry **78:**62-66

548   30.   **Roger M, Castelle C, Guiral M, Infossi P, Lojou E, Giudici-Orticoni M, Ilbert M.** 2012.

549   Mineral respiration under extreme acidic conditions: from a supramolecular organization to a

550   molecular adaptation in *Acidithiobacillus ferrooxidans*. Biochem Soc Trans **40:**1324

551   31.   **Yarzábal A, Brasseur G, Ratouchniak J, Lund K, Lemesle-Meunier D, DeMoss JA,**

552   **Bonnefoy V.** 2002. The high-molecular-weight cytochrome c Cyc2 of *Acidithiobacillus*

553   *ferrooxidans* is an outer membrane protein. J Bacteriol **184:**313-317

554   32.   **Liu W, Lin J, Pang X, Mi S, Cui S, Lin J.** 2013. Increases of ferrous iron oxidation activity and

555   arsenic stressed cell growth by overexpression of Cyc2 in *Acidithiobacillus ferrooxidans*

556   ATCC19859. Biotechnol Appl Biochem **60:**623-628

557   33.   **Jeans C, Singer SW, Chan CS, Verberkmoes NC, Shah M, Hettich RL, Banfield JF, Thelen**

558   **MP.** 2008. Cytochrome 572 is a conspicuous membrane protein with iron oxidation activity

559   purified directly from a natural acidophilic microbial community. ISME J **2:**542-

560   550.10.1038/ismej.2008.17.

561   34.   **Cury JA, Koo H.** 2007. Extraction and purification of total RNA from *Streptococcus mutans*

562   biofilms. Anal Biochem **365:**208-214

563   35.   **Bolger AM, Lohse M, Usadel B.** 2014. Trimmomatic: a flexible trimmer for Illumina sequence

564   data. Bioinformatics**:**btu170

565   36.   **Langmead B, Salzberg SL.** 2012. Fast gapped-read alignment with Bowtie 2. Nat Methods

566   **9:**357-359

567   37.   **Li H, Handsaker B, Wysoker A, Fennell T, Ruan J, Homer N, Marth G, Abecasis G, Durbin**

568   **R.** 2009. The sequence alignment/map format and SAMtools. Bioinformatics **25:**2078-2079

569   38.   **Robinson MD, McCarthy DJ, Smyth GK.** 2010. edgeR: a Bioconductor package for

570   differential expression analysis of digital gene expression data. Bioinformatics **26:**139-140

571   39.   **R Core Team.** 2014. R: A Language and Environment for Statistical Computing, v3.1.0. R

572   Foundation for Statistical Computing, Vienna, Austria. http://www.R-project.org/.

573   40.   **Benjamini Y, Hochberg Y.** 1995. Controlling the false discovery rate: a practical and powerful

574   approach to multiple testing. Journal of the Royal Statistical Society Series B

575   (Methodological)**:**289-300

576   41.   **McCarthy DJ, Chen Y, Smyth GK.** 2012. Differential expression analysis of multifactor RNA-

577   Seq experiments with respect to biological variation. Nucleic Acids Res**:**gks042

578   42.   **Robinson MD, Oshlack A.** 2010. A scaling normalization method for differential expression

579   analysis of RNA-seq data. Genome Biol **11:**R25

580   43.   **Kolde R.** 2013. pheatmap: Pretty Heatmaps, vR package version 0.7.7. http://CRAN.R-

581   project.org/package=pheatmap.

582   44.   **Pearson K.** 1895. Note on regression and inheritance in the case of two parents. Proceedings of

583   the Royal Society of London**:**240-242

584   45.   **Sullivan MJ, Petty NK, Beatson SA.** 2011. Easyfig: a genome comparison visualizer.

585   Bioinformatics **27:**1009-1010

586

587

26

588   Table 1. Sample and sequencing summary.

Sample ID[a]	Inoculum	Potential (mV vs. SHE) at sampling	Hours to max current	Max current (μA cm^{-2})	Current just before CV (μA cm^{-2})	Current at Sampling (μA cm^{-2})	E$_M$ (mV vs. SHE)	Reads passed QC	% reads unambiguously aligned
O1A	1	310	109	-50.2	-20.5	-35.3	440	16168243	37.9%
O1B	1	310	116	-31.9	-23.2	-29.3	460	15449422	46.7%
O2A	2	310	109	-14.3	-14.5	-12.6	480	4498496	61.5%
O2B	2	310	85	-13.4	-8.2	-8.44	500	9957581	69.4%
S1A	1	470	104	-54.3	-22.7	-7.29	420	13782405	65.1%
S1B	1	470	109	-64.1	-34.9	-23.6	450	11068839	68.7%
S2A	2	470	161	-53.5	-53.4	-52.2	430	15415038	87.5%
S2B	2	470	90	-14.9	-14.5	-19.6	454	13921246	80.5%

589   [a]Sample ID string {O=optimal (310 mV), S=suboptimal (470 mV)}{Inoculum 1 or 2}{replicate

590   A or B}

591

592

593
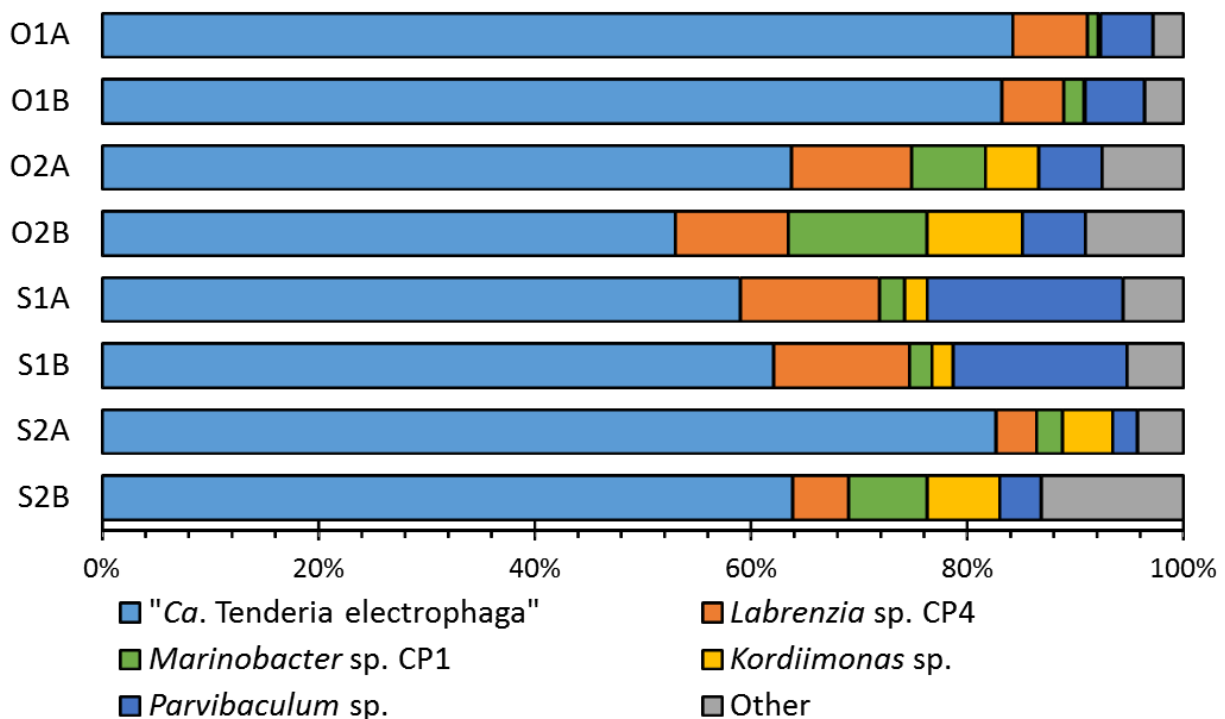
594   Figure 1. Relative activity of the five major constituents of Biocathode-MCL. Proportion of

595   reads matching a genome or bin normalized by the length of the genome or bin was taken as a

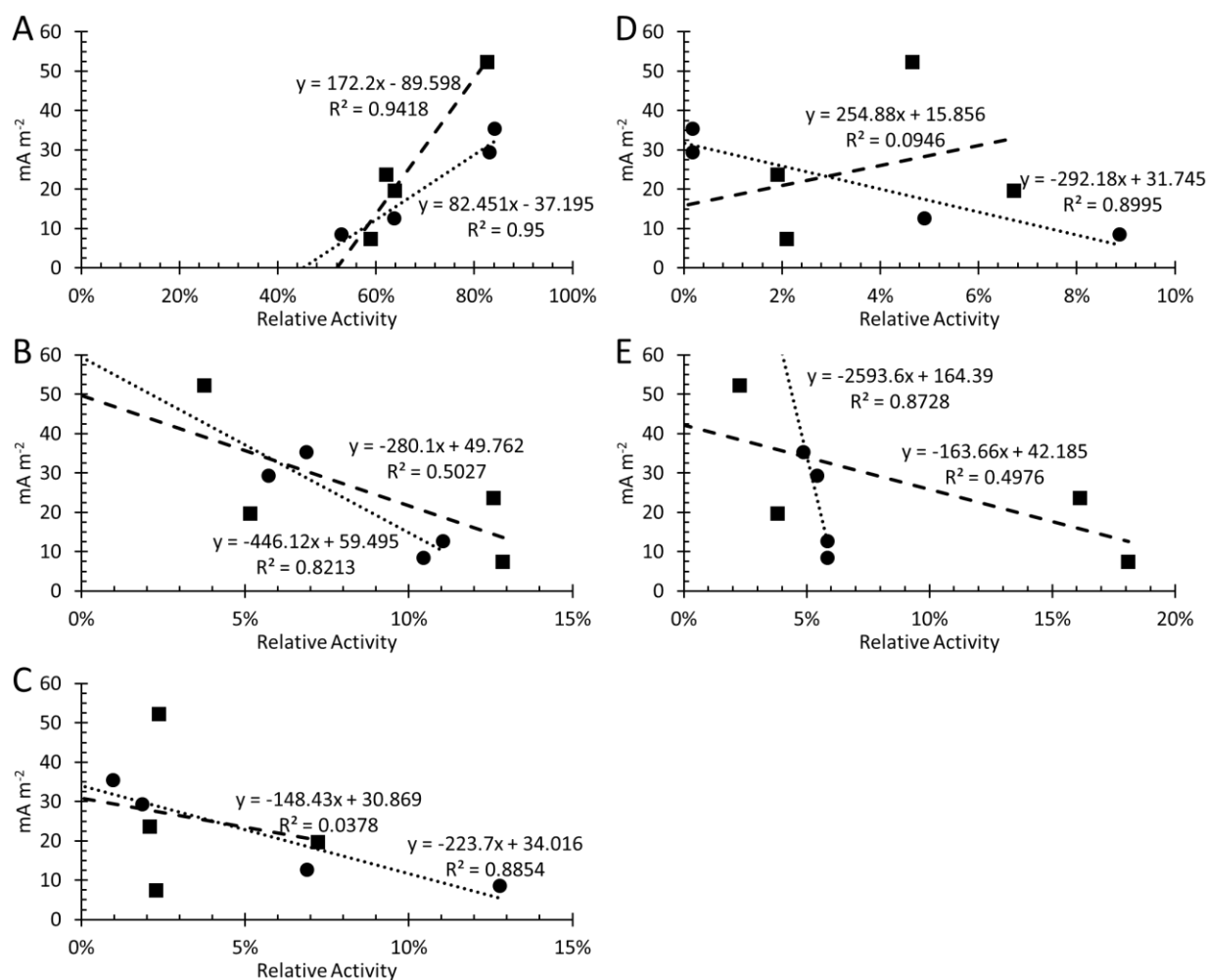596   proxy for activity. Sample labels are as in Table 1.

597

599 Figure 2. Activity of top five Biocathode-MCL constituents vs. current density at the optimal

600 and suboptimal electrodes potentials. *"Ca.* Tenderia electrophaga*"* (A) has positive correlations

601 with increasing negative current at both the optimal (circles) and suboptimal (squares) potentials.

602 Other active members of the community: *Labrenzia* sp. CP4 (B), *Marinobacter* sp. CP1 (C),

603 *Kordiimonas* sp. (D), and *Parvibaculum* sp. (E) had negative or insignificant correlation at both

604 potentials. Linear regression lines are shown, along with the equation of the lines and R^2 values.

605

606

607
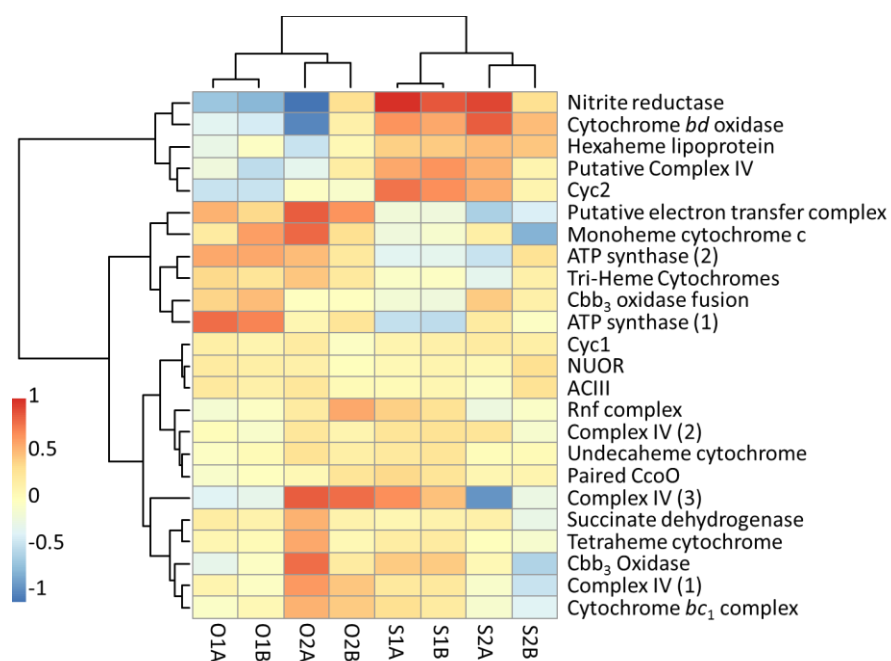
608   Fig. 3. Hierarchical clustering of EET and ETC components by change in expression.

609   Expression is normalized to 0 between biological replicates to focus on change in expression

610   between 310 mV and 470 mV. Details about genes in each complex are found in Table S1.
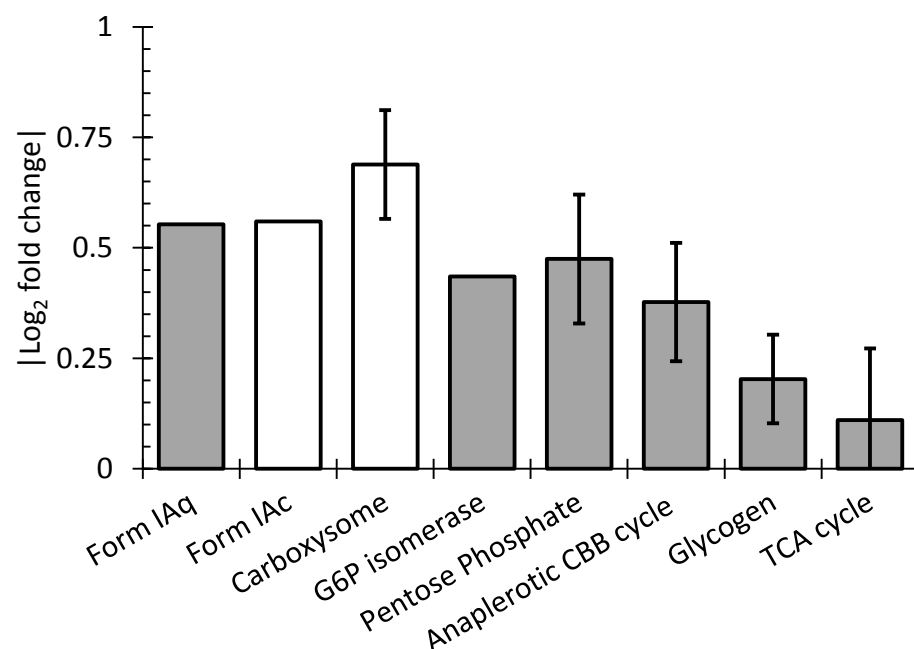
611   Sample identifiers are as in Table 1.

612

613

Fig. 4. Change in expression of central carbon metabolism genes. Open boxes are more highly expressed at 470 mV, gray boxes are more highly expressed at 310 mV. Error bars indicate standard deviation of $\log_2$ fold change of pathways containing three or more genes. Details of the genes included in each category, and their expression can be found in Table S3.
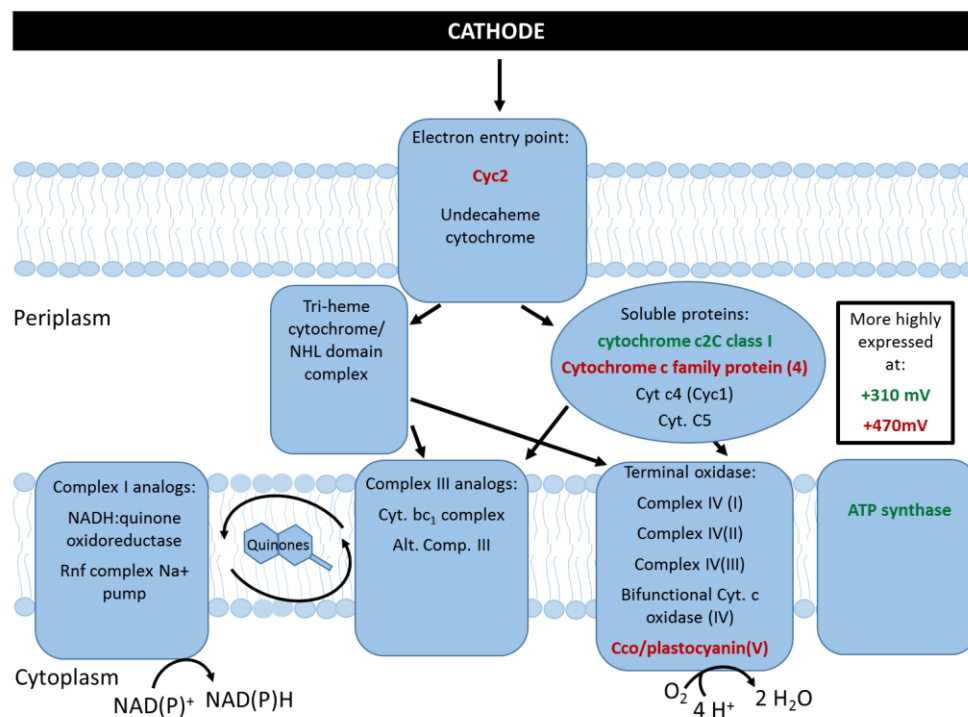
Fig. 5. Schematic of potential EET/ETC routes in "*Ca.* Tenderia electrophaga". Genes or complexes labeled in red are more highly expressed at 470 mV, those in green were more highly expressed at 310 mV.

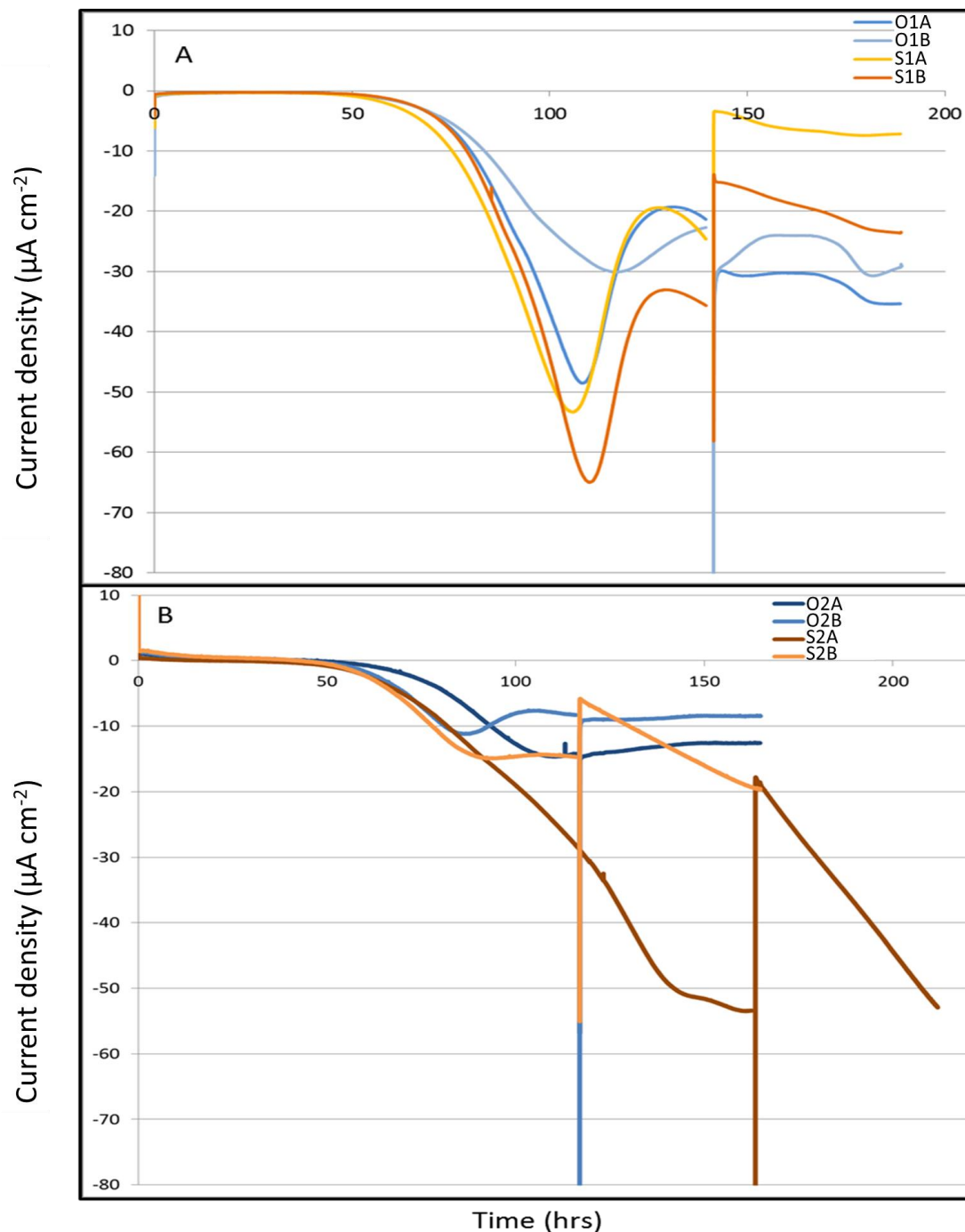625   Table S1. Expression of ETC components in "Ca. Tenderia electrophaga"

626   Table S2. ddPCR results

627   Table S3. Expression of central carbon metabolism genes in "Ca. Tenderia electrophaga"

628   Table S4. Expression of all annotated "Ca. Tenderia electrophaga" genes

629   Table S5. Primer sequences for ddPCR

630

631

Figure S1. Chromoamperometry of biofilms grown at the 310 mv and either switched to 470 mV

or continued at the optimal potential. Vertical lines indicate the time that the CV was measured

and potential was switched. Sample ID string {O=optimal (310 mV), S=suboptimal (470
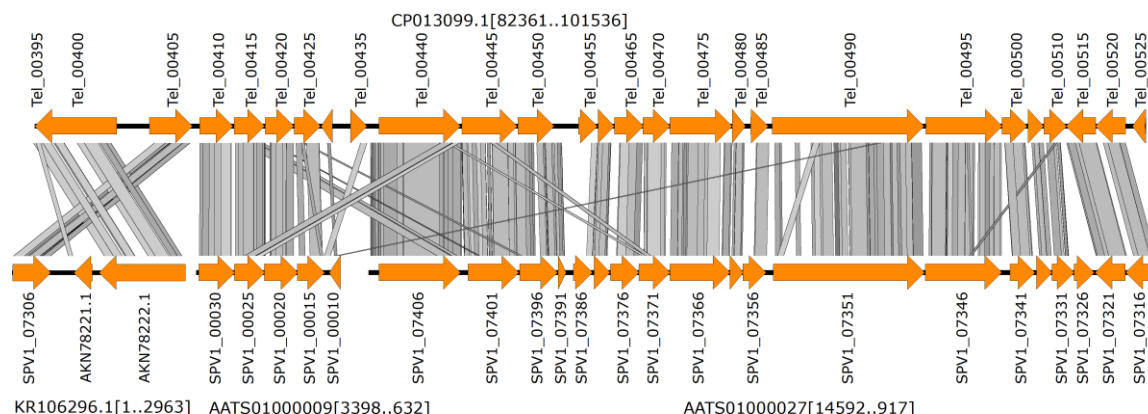
mV)}{Inoculum 1 or 2}{replicate A or B}.

34

636

637

638   Fig. S2 Synteny between "*Ca.* Tenderia electrophaga" and *Mariprofundus ferrooxydans* PV-1.

639   The *M. ferrooxydans* genes are found on three contigs in the NCBI database, but two

640   (KR106296.1 and AATS01000009) could be joined, as they have identical sequences at one end.

641   Gray lines indicate regions of homology determined by a tBlastx search in EasyFig 2.2.2 with e-

642   values of less than 1×10^{-13} with a minimum length of 30 bp (45). This region has been

643   previously noted by Barco et al. to be syntenous within neutrophilic iron oxidizing bacteria (19).

644

645